NASA TECHNICAL NOTE

NASA TN D-7534

"LIGHT BULB" HEAT EXCHANGER FOR MAGNETOHYDRODYNAMIC GENERATOR APPLICATIONS - PRELIMINARY EVALUATION

by J. Marlin Smith, Charles C. Hwang, and George R. Seikel

Lewis Research Center
Cleveland, Ohio 44135

NATIONAL AERONAUTICS AND SPACE ADMINISTRATION • WASHINGTON, D. C. • MARCH 1974

1. Report No. NASA TN D-7534	2. Government Accession No.	3. Recipient's Catalog No.
4. Title and Subtitle "LIGHT BULB" HEAT EXCHANGER FOR MAGNETOHYDRODYNAMIC GENERATOR APPLICATIONS - PRELIMINARY EVALUATION		5. Report Date March 1974
		6. Performing Organization Code
7. Author(s) J. Marlin Smith, Lewis Research Center; Charles C. Hwang, University of Pittsburgh, Pittsburgh, Pa.; and George R. Seikel, Lewis Research Center		8. Performing Organization Report No. E-7593
		10. Work Unit No. 503-10
9. Performing Organization Name and Address Lewis Research Center National Aeronautics and Space Administration Cleveland, Ohio 44135		11. Contract or Grant No.
		13. Type of Report and Period Covered Technical Note
12. Sponsoring Agency Name and Address National Aeronautics and Space Administration Washington, D.C. 20546		14. Sponsoring Agency Code

15. Supplementary Notes

16. Abstract

The light-bulb heat-exchanger concept is investigated as a possible means of using a combustion heat source to supply energy to an inert-gas MHD power generator system. In this concept, combustion gases flow through a central passage which consists of a duct with transparent walls through which heat is transferred by radiation to a radiation receiver which in turn heats the inert gas by convection. The effects of combustion-gas emissivity, transparent-wall transmissivity, radiation-receiver emissivity, and the use of fins in the inert-gas coolant passage are studied. The results indicate that inert-gas outlet temperatures of 2500 K are possible for combustion temperatures of 3200 K and that sufficient energy can be transferred from the combustion gas to reduce its temperature to approximately 2000 K. At this temperature more conventional heat exchangers can be used. Overall system efficiencies in the range of 50 percent appear possible, but this sensitivity depends upon the overall transmissivity of the transparent wall.

17. Key Words (Suggested by Author(s)) Magnetohydrodynamic power generation Radiant heat exchanger	18. Distribution Statement Unclassified - unlimited Cat. 33		
19. Security Classif. (of this report) Unclassified	20. Security Classif. (of this page) Unclassified	21. No. of Pages 27	22. Price* $3.00

"LIGHT BULB" HEAT EXCHANGER FOR MAGNETOHYDRODYNAMIC GENERATOR APPLICATIONS - PRELIMINARY EVALUATION

by J. Marlin Smith, Charles C. Hwang,[*] and George R. Seikel

Lewis Research Center

SUMMARY

The light-bulb heat-exchanger concept is investigated as a possible means of using a combustion heat source to supply energy to an inert-gas magnetohydrodynamic (MHD) power generator system. In this concept, combustion gases flow through a central passage which consists of a duct with transparent walls through which heat is transferred by radiation to a radiation receiver which in turn heats the inert gas by convection. The effects of combustion-gas emissivity, transparent-wall transmissivity, radiation-receiver emissivity, and the use of fins in the inert-gas coolant passage are studied. The results indicate that inert-gas outlet temperatures of 2500 K are possible for combustion temperatures of 3200 K and that sufficient energy can be transferred from the combustion gas to reduce its temperature to approximately 2000 K. At this temperature more conventional heat exchangers can be used. Overall system efficiencies in the range of 50 percent appear possible, but this sensitivity depends upon the overall transmissivity of the transparent wall.

INTRODUCTION

In the near term the only high-temperature heat source for magnetohydrodynamic (MHD) power generation appears to be combustion. A few authors have proposed the use of combustion in conjunction with some form of heat exchanger to provide the high temperatures required for the inert-gas MHD generator. The basic advantages of this configuration, as compared to directly utilizing the combustion gases as the working fluid in the generator, appear to be higher power density, lower rejection temperature, and overcoming the corrosion and seed contamination problems associated particularly with the use of "dirty" combustion fuels.

---

[*] Professor of Mechanical Engineering, University of Pittsburgh, Pittsburgh, Pa.

The major problem in developing such a heat exchanger lies in the high combustion temperature (~3200 K), which requires the use of refractory metals, while the abundance of free oxygen and hydrogen in the combustion gases is incompatible with the use of refractory metals. Therefore, a means of using refractory metals is needed which would keep the highly corrosive combustion gases away from the metal surfaces. One such means would be the injection of an inert gas along the surface. The obvious disadvantage of this scheme is the expense or the need for recovery of the inert gas.

We therefore are considering the possibility of using a heat-exchanger concept developed for gas-core nuclear rockets (ref. 1). This concept as it applies to the MHD system is shown in figure 1. The combustion gases flow through the central passage, which consists of a duct with transparent walls through which heat is transferred by radiation to a radiation receiver which in turn heats the inert gas by convection. This device, for obvious reasons, is called a "light bulb" heat exchanger.

Since the transparent wall is not transparent to all frequencies, some of the radiant energy is absorbed. In addition, the convective heat from the combustion gas is transferred to the wall. Therefore, the wall must be cooled (to ~1000 K). Furthermore, the combustion products must be kept from coating the wall and making it opaque. We therefore contemplate scavenging the transparent wall with oxygen or oxygen-enriched air. The final combustion condition is then brought to stoichiometric either by initially running the combustion process fuel rich or by the addition of supplementary fuel in or after the radiant heat exchanger.

The development of such a heat exchanger at power levels required for commercial power applications may be a formidable undertaking. In this report only the feasibility of such a device for MHD applications is considered. The study is limited to the determination of the net heat transfer as a measure of the physical size of the device and whether this is sufficient to heat the inert gas to 2500 K while cooling the combustion gases to temperatures where more conventional heat exchangers can be used (e.g., a pebble-bed heat exchanger, which operates at $\lesssim$ 2300 K). A block diagram of the overall system studied in this report is shown in figure 2.

ANALYSIS

Assumptions

The configuration of the "light bulb" heat exchanger used in this study is shown in figure 1. In order to make the analysis tractable, we assume that sufficient coolant can be provided to cool the transparent wall and to provide the buffer flow between this wall and the combustion gas. In the nuclear light-bulb theoretical design (ref. 1), sufficient

cooling is achieved at five times the heat flux obtained in this analysis. We therefore consider the transparent wall to be a single wall.

We further assume that a buffer of low-velocity inert gas can be provided between the transparent wall and the radiation receiver with minimal heat transfer to and from the containing walls. This buffer will probably be required in order to minimize the pressure differential across the transparent wall. In practice, this region would be the first pass for the inert gas through a double-pass heat exchanger, as shown in figure 1. With these assumptions we approximate the actual configuration by that shown in figure 3. To simplify the calculation of the heat transfer from the combustion gas to the inert gas, the region between the transparent wall and the radiation receiver is treated as a vacuum.

Other assumptions used in the analysis are as follows:

(1) The heat transfer in the axial direction is small compared with that in the radial direction.

(2) The combustion gas is a gray body with constant emissivity and radiates at the combustion temperature of the gas.

(3) The transparent wall is at a constant temperature T_1. The transmissivity of the wall is constant between $\lambda_{min} \leq \lambda \leq \lambda_{max}$ and zero elsewhere.

(4) The conditions in the system are steady.

(5) The radiation receiver is treated as a gray body with constant emissivity with respect to temperature.

(6) Gas dynamic quantities vary only in the axial direction.

Heat-Transfer Equations

The optical properties of the various members of the heat exchanger are listed here. All values of reflectivity r, absorptivity α, and transmissivity τ are taken to be constant over their defined wavelengths. Furthermore, from Kirchoff's law, the emissivity ϵ is equal to the absorptivity. The reflectivity is assumed to be diffuse. The optical parameters are taken to be as follows:

Combustion gas:

$$\alpha_g + \tau_g = 1 \qquad \epsilon_g = \alpha_g \qquad r_g = 0$$

3

Transparent wall:

$$\alpha_1 + \tau_1 = 1 \quad \epsilon_1 = \alpha_1 \quad r_1 = 0 \quad \text{for } \lambda_{min} \leq \lambda \leq \lambda_{max}$$

$$\alpha_1 = \epsilon_1 = 1 \quad \tau_1 = r_1 = 0 \quad \text{for } \lambda_{min} \geq \lambda \geq \lambda_{max}$$

Radiation receiver, surfaces $j = 2, 3, 4$:

$$\alpha_2 = \alpha_3 = \alpha_4 \quad r_2 = r_3 = r_4 \quad \tau_2 = \tau_3 = \tau_4$$

$$\alpha_j + r_j = 1 \quad \epsilon_j = \alpha_j \quad \tau_j = 0$$

Inert gas:

$$\alpha_i = r_i = \epsilon_i = 0 \quad \tau_i = 1$$

With these properties and for the infinitely long concentric cylinder geometry shown in figure 3, the net radiant heat transfer to or from each of the elements of the heat exchanger can, with considerable algebraic effort, be derived by any of a number of standard techniques available in texts on heat transfer. The net radiant heat flux from the combustion gas q_{gr}, into the transparent wall q_{1r}, and into the radiation receiver q_{2r} are, respectively,

$$q_{gr} = \epsilon_g \left[\left(\sigma T_g^4 - H_g \right) - \left(\sigma T_1^4 - H_1 \right) \right]$$

$$+ \epsilon_g \frac{\left[\epsilon_2 + (1 - \epsilon_2)\left(1 - \tau_1^2\right)\dfrac{R_g}{R_2} \right](H_g - H_1) - \epsilon_2 \tau_1 (H_2 - H_1)}{\epsilon_2 + (1 - \epsilon_2)\left[1 - (1 - \epsilon_g)\tau_1^2 \right]\dfrac{R_g}{R_2}} \tag{1}$$

$$q_{1r} = \epsilon_g\left[\left(\sigma T_g^4 - H_g\right) - \left(\sigma T_1^4 - H_1\right)\right] + \epsilon_2 \frac{\left[\left(\sigma T_2^4 - H_2\right) - \left(\sigma T_1^4 - H_1\right)\right]}{\left[\epsilon_2 + (1 - \epsilon_2)\dfrac{R_g}{R_2}\right]}$$

$$+ (1 - \tau_1)\frac{\epsilon_g\left[\epsilon_2 + (1 + \tau_1)(1 - \epsilon_2)\dfrac{R_g}{R_2}\right](H_g - H_1)}{\epsilon_2 + (1 - \epsilon_2)\left[1 - (1 - \epsilon_g)\tau_1^2\right]\dfrac{R_g}{R_2}}$$

$$+ (1 - \tau_1)\frac{\epsilon_2\left[1 + \tau_1(1 - \epsilon_g)\right](H_2 - H_1)}{\epsilon_2 + (1 - \epsilon_2)\left[1 - (1 - \epsilon_g)\tau_1^2\right]\dfrac{R_g}{R_2}} \qquad (2)$$

$$q_{2r} = -\frac{\epsilon_2\left(\dfrac{R_g}{R_2}\right)}{\left[\epsilon_2 + (1 - \epsilon_2)\dfrac{R_g}{R_2}\right]}\left[\left(\sigma T_2^4 - H_2\right) - \left(\sigma T_1^4 - H_1\right)\right]$$

$$+ \frac{\epsilon_2\left(\dfrac{R_g}{R_2}\right)\left\{\tau_1\epsilon_g(H_g - H_1) - \left[1 - \tau_1^2(1 - \epsilon_g)\right](H_2 - H_1)\right\}}{\epsilon_2 + (1 - \epsilon_2)\left[1 - (1 - \epsilon_g)\tau_1^2\right]\dfrac{R_g}{R_2}} \qquad (3)$$

where H is the total emissive power of a black body between λ_{min} and λ_{max} and σ is the Stefan-Boltzmann constant.

Referring again to figure 3, there is additional radiant heat transfer across the inert-gas coolant passage. The net radiant heat flux into the cool side of the radiation receiver from the hot side is given by

$$q_{4r} = \frac{\epsilon_3\sigma\left(T_3^4 - T_4^4\right)}{2 - \epsilon_3} \qquad (4)$$

5

where it has been assumed that $R_3/R_4 \simeq 1$.

In order to completely specify the heat balance, there are, in addition to the preceding radiant heat fluxes, a convective heat flux from the combustion gas to the transparent wall, cooling of the transparent wall, heat conduction through the inner wall of the radiation receiver to the inert gas, and a convective heat flux into the inert gas from both the hot and cool sides of the radiation receiver. In this analysis we assume that the transparent wall can be cooled and maintained at a constant temperature $T_1 \simeq 1000$ K. It is presumed that the convective heat flux from the combustion gas would be removed by transpiration cooling, which would also provide the buffer between the combustion gas and the transparent wall. The radiation absorbed by the wall would be removed by internal cooling passages. The outer wall of the radiation receiver is assumed to be thermally insulated so that there is no heat transfer through this wall. The convective heat flux from the combustion gas is

$$q_{gc} = h_g(\overline{T}_g - T_1) \tag{5}$$

where h_g is the film coefficient and $\overline{T}_g$ is the recovery temperature.

Similarly, the convective heat fluxes into the inert gas from the hot and cool walls of the radiation receiver are, respectively,

$$q_{3c} = \eta h_3(T_3 - \overline{T}_{i3}) \tag{6}$$

$$q_{4c} = \eta h_4(T_4 - \overline{T}_{i4}) \tag{7}$$

where the h's are taken to be the smooth-pipe film coefficients and η takes into account the extended heat-transfer surface introduced by the use of fins.

Finally, the heat flux through the inner wall of the radiation receiver is given by

$$q_{23} = \frac{K}{W_{23}} (T_2 - T_3) \tag{8}$$

where K is the thermal conductivity of the wall material and W_{23} is the wall thickness.

Gas Dynamic Equations

In general, the gas dynamic equations for the axial variation of temperature and pressure in a constant-area duct take the form

6

$$(1 - M^2)\frac{1}{T}\underline{v}\cdot\overline{\nabla}T = \frac{-(1 - \gamma M^2)\delta Q + (\Lambda_P - 1 + \gamma M^2)\underline{v}\cdot\delta\underline{X}}{\rho C_P T} \tag{9}$$

$$\frac{\gamma - 1}{\gamma}(1 - M^2)\frac{1}{P}\underline{v}\cdot\overline{\nabla}P = \frac{-(\gamma - 1)M^2\dfrac{\Lambda_P}{\Lambda_T}\delta Q - \dfrac{\Lambda_P^2}{\Lambda_T}\left[1 + \dfrac{(\gamma - 1)M^2}{\Lambda_P}\right]\underline{v}\cdot\delta\underline{X}}{\rho C_P T} \tag{10}$$

where δQ is the ratio of the volume heat loss to the unit volume and $\delta\underline{X}$ is the ratio of the friction force to the unit length.

$$\Lambda_P \equiv -\left.\frac{\delta \ln\rho}{\delta \ln T}\right|_P \tag{11}$$

$$\Lambda_T \equiv -\left.\frac{\gamma \ln\rho}{\gamma \ln T}\right|_T \tag{12}$$

Additional symbols are defined in the appendix.

To avoid the relatively complicated computation of combustion gas transport properties, the following assumptions are made:

(1) In the calculations carried out in this analysis the velocity of the combustion gas is very slow ($M_g < 0.01$). We therefore nelgect the effect of friction on the combustion gas flow.

$$\delta\underline{X}_g = 0 \tag{13}$$

(2) The convective heat flux from the combustion gas to the transparent wall is reduced to zero by transpiration cooling, and the transpirant keeps the wall clean. For this condition,

$$q_{gc} = 0 \tag{14}$$

The net volume heat loss δQ_g from the combustion gas in the incremental length dx is then just the net radiant heat flux q_{gr} times the area $2\pi R_1\, dx$ divided by the gas volume $\pi R_1^2\, dx$.

$$\therefore \delta Q_g = \frac{2q_{gr}}{R_1} \tag{15}$$

7

The friction force per unit length for the inert gas is taken to be that of a smooth pipe increased by the extended area factor η

$$\delta \underline{X}_i = -\eta f \frac{\rho v}{W_i} \underline{v} \tag{16}$$

where f is the smooth-pipe friction factor.

Since the outer wall of the radiation receiver is thermally insulated, the net heat flux into the inert gas is just equal to the net radiant heat flux q_{2r} to the radiation receiver. The net heat $-\delta Q_i$ into the inert gas in the incremental length dx is then just the flux q_{2r} times the area $2\pi R_2 \, dx$ divided by the gas volume $\simeq 2\pi R_2 W_{34} \, dx$.

$$\therefore \delta Q_i = -\frac{q_{2r}}{W_{34}} \tag{17}$$

Substituting equations (13) and (15) into equations (9) and (10) yields the following equations for the axial temperature and pressure variation of the combustion gas:

$$\frac{dT_g}{dx} = -\frac{1 - \gamma_g M_g^2}{1 - M_g^2} \frac{2\pi R_1 q_{gr}}{\dot{m}_g (C_P)_g} \tag{18}$$

$$\frac{dP_g}{dx} = -\frac{\gamma_g M_g^2}{1 - M_g^2} \frac{\Lambda_P}{\Lambda_T} P_g \frac{2\pi R_1 q_{gr}}{\dot{m}_g (C_P)_g T_g} \tag{19}$$

where the combustion gas is assumed to flow in the positive X-direction.

Substituting equations (16) and (17) into equations (9) and (10) yields the following equations for the axial temperature and pressure variation of the inert gas:

$$\frac{dT_i}{dx} = -\frac{\left[\dfrac{1 - \gamma_i M_i^2}{1 - M_i^2} 2\pi R_2 q_{2r} - \dfrac{\gamma_i M_i^2}{1 - M_i^2} 2\pi R_2 \eta f \rho_i v_i^3\right]}{\dot{m}_i (C_P)_i} \tag{20}$$

$$\frac{dP_i}{dx} = P_i \frac{\dfrac{\gamma M_i^2}{1 - M_i^2} 2\pi R_2 q_{2r} + \dfrac{\gamma_i}{\gamma_i - 1} \dfrac{1 + (\gamma_i - 1)M_i^2}{1 - M_i^2} 2\pi R_2 \eta f \rho_i v_i^3}{\dot{m}_i (C_P)_i T_i} \qquad (21)$$

where the friction factor $f = 0.046$ (Reynolds number)$^{-0.2}$ is evaluated at the average Reynolds number between the hot and cool sides of the radiation receiver, and the inert-gas flow is taken to be in the negative X-direction.

Method of Solution

The problem of interest here is the determination of the combustion and inert gas properties as a function of axial position along the heat exchanger. This determination is accomplished by numerical integration of equations (18) to (21) by the Runge-Kutta-Merson method (ref. 2). This method requires solving the combustion chemistry and heat balance at each axial station along the heat exchanger. In order to do this, we specify the geometrical sizes of the heat exchanger; the optical properties; the transparent wall temperature; the inlet Mach number, stagnation pressure, and stagnation temperature of the combustion gas; and the outlet Mach number, stagnation pressure, and stagnation temperature of the inert gas.

Having specified the initial temperature and pressure of the combustion gas and calculating the temperature and pressure at each station by the numerical integration of equations (18) and (19) allow the combustion chemistry to be solved as a temperature-pressure problem by the method of reference 3. The radiant heat fluxes (eqs. (1) to (3)) can be calculated once the temperature T_2 is determined from the following equations:

$$q_{2r}(T_g, T_1, T_2) = q_{23}(T_2, T_3) \qquad (22)$$

$$q_{23}(T_2, T_3) = q_{3c}(T_3, \overline{T}_{i3}) + q_{4c}(T_4, \overline{T}_{i4}) \qquad (23)$$

$$\eta h_4(T_4 - \overline{T}_{i4}) = \frac{\epsilon_3 \sigma \left(T_3^4 - T_4^4\right)}{2 - \epsilon_3} \qquad (24)$$

Equation (22) states that the heat flux through the inner wall of the radiation receiver must equal the net radiant flux to the receiver (eqs. (3) and (8)). Equation (23) states that the heat flux into the inert gas must equal the heat flux through the inner wall of the

9

radiation receiver (eqs. (6) and (8)). Equation (24) states that the heat flux into the inert gas from the cool wall of the radiation receiver is equal to the radiant heat flux from the hot to the cool side of the inert gas channel (eqs. (4) and (7)).

For inert gases the Prandtl number is approximately 1. To simplify the calculations, the Prandtl number is therefore taken to be 1 and then the recovery temperatures $(\overline{T}_{i3}, \overline{T}_{i4})$ are just the stagnation temperature of the inert gas. The film coefficients h are of the form

$$h = 0.02 \frac{K}{W_{34}} \text{ (Reynolds number)}^{0.8} \tag{25}$$

and are evaluated at a temperature midway between their respective wall temperatures and the recovery temperature. The thermal conductivity and viscosity for argon were calculated for Lennard-Jones 6-12 potential from the data of reference 4. Equation (24) can be solved explicitly for T_3, which substituted into equations (22) and (23) yields two nonlinear integral equations (integration over wavelengths) for T_2 and T_4:

$$q_{2r}(T_g, T_1, T_2) = q_{23}(T_2, T_1, T_4) \tag{26}$$

$$q_{23}(T_2, T_1, T_4) = q_{3c}(T_4, T_1) + q_{4c}(T_4, T_1) \tag{27}$$

These two equations must then be solved by some iterative procedure. The method used in this analysis is based on the fact that the integration method used to solve the temperature and pressure equations (20) and (21) results in small changes in all quantities from station to station. Therefore, the unknown values of T_2 and T_4 at station $N + 1$ are just the known values at N plus some small change, that is,

$$T_{2_{N+1}} = T_{2_N} + \delta T_2 \tag{28}$$

$$T_{4_{N+1}} = T_{4_N} + \delta T_4 \tag{29}$$

Substituting equations (28) and (29) into equations (26) and (27) and retaining only linear terms in δT_2 and δT_4 yield two linear equations for these quantities which are easily solved to yield

$$\delta T_2 = \delta T_2\left(T_{g_{N+1}}, T_{1_{N+1}}, T_{2_N}, T_{i_{N+1}}, T_{4_N}\right) \tag{30}$$

$$\delta T_4 = \delta T_4\left(T_{g_{N+1}}, T_{1_{N+1}}, T_{2_N}, T_{i_{N+1}}, T_{4_N}\right) \tag{31}$$

Since all the temperatures are known, δT_2 and δT_4 can be calculated and new values for T_2 and T_4 are then determined from equations (28) and (29). The correctness of these values is checked by evaluating equations (26) and (27) and comparing the values on the left and right sides. If the left and right sides of both equations agree to within the desired accuracy, the solutions are correct. If not, the new values of T_2 and T_4 are substituted into equations (30) and (31) and the procedure is repeated until the desired accuracy is obtained. The temperature T_4 can then be calculated from equation (24). Then all temperatures are known. The heat fluxes needed in equations (18) to (21) can be calculated and the integration can be carried out to the next station. In general, three to five iterations are required to obtain accuracy to three significant figures.

The only problem in this iterative procedure is in starting the procedure at the first station. The problem obviously arises because we have no previous station upon which to base our initial estimates of T_2 and T_4. In general, the iterative method will converge for any initial choice of T_2 and T_4. However, the speed with which it converges, that is, the number of iterations, depends upon how close the first guess is to the true solution. We therefore find it convenient to take the initial estimate of T_2 as the value midway between the specified inlet combustion-gas temperature T_g and the specified outlet inert-gas temperature T_i, that is,

$$T_2\Big|_{\text{initial}} = \frac{T_g + T_i}{2} \tag{32}$$

The initial estimate of T_4 is taken to be midway between the hot-wall temperature T_3 and the specified inert-gas temperature. Since T_3 is not initially specified, it is taken to be midway between T_2 (eq. (32)) and the specified inert-gas temperature. The initial estimate of T_4 is therefore

$$T_4\Big|_{\text{initial}} = \frac{1}{8} T_g + \frac{7}{8} T_i \tag{33}$$

DISCUSSION OF RESULTS

Selection of Initial Conditions and Heat-Exchanger Geometry

The initial conditions and geometry of the light-bulb heat exchanger which have been

analyzed in this report have been chosen rather arbitrarily. Therefore, the results are probably not the most optimistic obtainable. The choices which were made and the reasons are as follows:

(1) The inlet pressure of the combustion gas and the outlet pressure of the inert gas were taken to be 10 atmospheres. This pressure level was chosen as a compromise between obtaining high convective heat transfer into the inert gas and keeping the pressure low enough for effective MHD generator operation with presently available magnetic field strength. The combustion gas was taken to be at the same pressure level in order to minimize the pressure differential across wall structures. This procedure allows thin walls for maximum heat transfer.

(2) The combustion was stoichiometric and the fuel was the char formulation $(CH_{0.182}O_{0.015})$ of reference 5 with a heat value of 33.54 MJ/kg. Stoichiometric burning was a purely arbitrary choice. The fuel was chosen on the basis that the near black body radiation of luminous gases is a result of radiation from unburned carbon particles. Therefore, burning high-carbon fuels is advantageous.

(3) The inlet stagnation temperature of the combustion gas was taken to be 3200 K. For the preceding stoichiometric conditions the flame temperature is approximately 3580 K. Obviously, since the heat transfer is radiative, the higher the temperature, the more effective is the heat-transfer process and nearly in direct proportion to T^4. However, there are heat losses in the combustor. Furthermore, if we are to obtain a luminous gas from unburned carbon particles, the combustion in the combustor cannot be 100 percent efficient. Lastly, we may want to burn fuel rich in order to obtain the unburned carbon particles or to make up for whatever oxygen is used to scavenge the transparent wall. While these considerations lower the input combustion gas temperature, it is not clear how to use the heat which is removed from the transparent wall. One way is to use this heat to provide oxygen preheat, which increases the temperature. Obviously, the answer to these questions depends upon a detailed systems analysis. Therefore, the choice of 3200 K was considered as a conservative estimate between what ideally could be obtained and what realistically will be obtained.

(4) The radius of the combustion gas channel R_1 was taken to be 1 meter and the inlet Mach number 0.01. This choice gives a thermal input of 345 megawatts. Six such heat exchangers would yield 1000 megawatts of electric output at 50 percent efficiency. This number represents a compromise between the simplicity of one large heat exchanger and the desirability of a number of smaller heat exchangers. Use of several exchangers is desirable since this increases the surface-volume ratio upon which the effectiveness of the heat-transfer process is based. The particular combination of R_1 and Mach number chosen here was a compromise between size and the desire to minimize the convective heat loss to the transparent wall. For the cases considered the convective heat transfer is, at worst, approximately 10 to 30 percent of the radiative

heat transfer absorbed by the transparent wall.

(5) The thickness of the inner wall of the radiation receiver W_{23} was taken to be 0.25 centimeter. The thermal conductivity of the two likely candidates for wall material (graphite and tungsten) is approximately 1 W/cm/K in the temperature range of interest. The maximum heat flux through the wall is approximately 100 W/cm^2. Therefore, the temperature drop is approximately 100 K per centimeter of thickness. Obviously even at more reasonable thicknesses (particularly for graphite), the temperature drop through the inner wall of the radiation receiver is small in comparison to the 700 K temperature drop between the combustion gas and the inert gas. For the thickness used, the temperature drop across the wall was found to have little effect upon the heat transfer.

(6) To effect high radiant heat transfer at the temperatures considered herein, it is necessary to maintain a high temperature differential between the combustion gas and the radiation receiver. Thus, we must minimize the temperature drop between the radiation receiver and the inert gas if we are to obtain a high inert gas temperature. Since the radiant heat flux from the combustion gas to the radiation receiver drops off as R_1/R_2, it is obvious that the farther the radiation receiver is removed from the combustion-gas channel, the less the heat flux to the radiation receiver and hence the smaller the temperature drop between the radiation receiver and the inert gas. In the cases considered herein, R_2 was taken to be 3 meters, that is, $R_1/R_2 = 1/3$. This choice was a compromise between the desire to obtain large radiant heat fluxes from the combustion gas and reasonable overall sizes for the heat exchanger.

(7) The outlet stagnation temperature of the inert gas was taken to be 2500 K. An inert-gas temperature in this range seems necessary in order to make the efficiency of the inert-gas MHD system attractive relative to directly extracting the power with a combustion-gas MHD system.

(8) By setting the combustion-gas inlet conditions we have set the mass flow. Then, just as in an ordinary heat exchanger, there is an inert-gas mass flow necessary to maintain the heat transfer through the heat exchanger. Since the stagnation temperature and pressure have been chosen, the mass flow is obtained by proper selection of Mach number M_i and channel width W_{34}. Obviously, the mass flow is directly proportional to both. However, the friction loss increases with Mach number and decreases with width. A reasonable compromise occurs for $M_i = 0.12$ and $W_{34} = 6$ centimeters.

Results of Selected Cases

Perhaps the greatest problems in ascertaining the feasibility of the light-bulb heat exchanger lie in the uncertainty in estimating realistic optical properties and the numer-

ical difficulty of including them in the calculation system. In this section we investigate the effect that various values of these properties have upon the heat transfer and probable efficiency of the thermodynamic system.

A schematic of the thermodynamic cycle to be discussed is shown in figure 2. It is based on the following assumptions: from reference 6 it appears that an inert-gas MHD-turbine cycle with a peak temperature of 2500 K can reach an efficiency of 60 percent or greater and that the initial temperature at which heat is added to the inert gas is approximately 850 K. We therefore assume that the heat input to the inert gas raises its temperature from 850 K to 2500 K and that this heat can be converted at 60 percent efficiency. Since the combustion gas still contains a large amount of heat after leaving the inert-gas-loop heat exchangers, a bottoming cycle of some form is required in order to provide a high overall system efficiency. We assume that this heat can be converted with an efficiency of 40 percent.

The various cases considered and their parametric variation are listed in table I. (The combustion and inert gases flow counter to one another.) Case 1 is for the initial conditions given in the previous section and is referred to as the ideal case since the optical properties selected are assumed to be the most ideal. That is, the combustion gas radiates as a black body; the optical window of the transparent wall between λ_{min} and λ_{max} is totally transparent, λ_{max} = 4.2 micrometers (the optimism of this selection will be discussed later); the radiation receiver is a black body; and fins can be designed to increase the effective heat-transfer area in the inert-gas channel by a factor of 5. Case 1 is the ideal case to which the others are compared.

The blanks in table I mean that the values are the same as for the ideal case. Two efficiency values are given in the last column for each case. The upper value assumes that the heat transferred to the transparent wall can be converted in the bottoming cycle, while the lower value assumes that it is totally lost.

The results for cases 1 and 2 are shown in figure 4. Obviously, for both cases the goal of attaining an inert-gas outlet temperature of 2500 K while reducing the combustion-gas temperature to a value (~ 2000 K) at which more conventional heat exchangers operate can be achieved.

Figure 4 shows a rapid leveling off of the inert-gas temperature beyond 10 to 12 meters. This leveling off reflects the strong T^4 temperature dependency of the radiation heat transfer, which becomes increasingly ineffective at lower temperature. Another effect is the increasing fraction of the radiant energy from the combustion gas which is absorbed by the transparent wall. This results from the fact that, as the combustion gas and the radiation receiver cool, their radiation spectrum shifts farther and farther into the infrared. A greater fraction of the energy then lies beyond the infrared cutoff (λ_{max} = 4.2 μm) of the transparent wall and hence is absorbed. These trends yield a length beyond which the heat exchanger can be considered ineffective. This

14

length is arbitrarily chosen to be 15 meters. All other cases will be compared with the ideal case for this length.

At the 15-meter length the inert-gas inlet temperature is 1400 K. Therefore, in order to bring the temperature down to the 850 K for which the efficiency is calculated, an additional heat exchanger (referred to as optional conventional heat exchanger - fig. 2) between the combustion gas and the inert gas is required. The other alternative (chosen for case 2) is to reduce the mass flow of the inert gas such that all the thermal input to the inert gas is taken through the light-bulb heat exchanger. This was accomplished by reducing the Mach number to 0.102 and the channel width to 5.1 centimeters. The result (shown by the dashed curves in fig. 4) is that less of the thermal input of the combustion gas is converted in the MHD loop and hence the overall efficiency of the system is reduced. This decrease in efficiency is approximately 3.5 points, as shown in table I. However, it should be pointed out that the pressure drop has been reduced by approximately 20 percent, not even including the drop across the second heat exchanger required in case 1. This lower pressure drop results in less pumping power as compared to case 1 and hence increases the efficiency relative to that case. The size of this increase requires a more extensive systems analysis.

Figure 5 shows the effect of decreasing the combustion-gas emissivity ϵ_g to 0.6. The circular symbols shown at 15 meters on this and succeeding figures refer to the values obtained in case 1. The solid curves refer to the conditions of case 1 but with an emissivity equal to 0.6. The temperature drops obtained in case 1 at 15 meters can be obtained in this case by increasing the heat-exchanger length to approximately 24 meters. However, the pressure drop is increased because of the increased duct length. The dashed curves in figure 5 refer to case 3, in which the mass flow of the combustion gas is decreased by decreasing its Mach number to 0.007 and the mass flow of the inert gas is decreased by decreasing its Mach number to 0.102 and its channel width to 4.8 centimeters. This case yields approximately the same results as obtained in case 1. However, the thermal input is now lower and hence more heat exchangers are required to obtain the 1000 megawatts of power output. Lowering the emissivity therefore increases the size of the heat exchanger.

Figure 6 shows the effect of decreasing the transmissivity of the optical window of the transparent wall τ_1 to 0.9. The solid curves show the results for the gas flow conditions of case 1. The obvious result occurs. The transparent wall absorbs a greater fraction of the energy radiated from the combustion gas. The inert gas receives very little of the energy, and at 15 meters the temperature difference is so small that very little energy is transferred.

The dashed lines on figure 6 represent case 4 of table I. The mass flow of the inert gas is decreased by decreasing the Mach number to 0.108 and the channel width to 5.4 centimeters. This case yields nearly the same temperature and pressure drops as

case 1. However, the fraction of power radiated to the transparent wall is nearly three times as great. As noted in table I the effect upon overall efficiency is not critical if the power absorbed by the transparent wall can be recovered in the bottoming cycle. However, if recovery cannot be made, there is little to be gained by the incorporation of the MHD loop since the bottoming cycle is already 40 percent efficient.

Figure 7 shows the effect of decreasing the infrared cutoff τ_{max} to 3 micrometers. The results are similar to those obtained in the previous case. However, the shift of the cutoff from 4.2 to 3 micrometers is not great and hence indicates the importance of this cutoff. This cutoff will be particularly critical if the unburned carbon particles, and hence a luminous gas, cannot be maintained throughout the heat-exchanger length. In that case one must rely increasingly on the radiation of H_2O and CO_2 bands. The effective emissivity of these gases may be in the range of 0.2 to 0.4 (see section 38-6 of ref. 7), which from the results of case 3 would indicate that the sole effect would be to increase the size of the heat exchanger. However, the spectrum of these bands does not fill the black body spectrum and, in fact, lies near the infrared cutoff of the transparent wall. Hence, a greater fraction of this radiation will be absorbed, leading not only to larger sizes but to lower efficiencies.

Another effect which has not been included in this analysis is the effect of the shift in the black body spectrum of the combustion gas toward the infrared (ch. 11, ref. 8). This shift is caused by the thermal gradient which must exist between the hot core of the gas and the cold transparent wall. The effect of this shift upon the overall performance of the cycle obviously critically depends upon the infrared cutoff.

Figure 8 shows that the effect of decreasing the emissivity of the radiation receiver ϵ_r to 0.9 is negligible.

Figure 9 shows the effect of decreasing the factor accounting for the effective heat-transfer area produced by fins η from 5 to 2.5. The effect is similar to that caused by decreasing the emissivity of the combustion gas (fig. 4). The size of the heat exchanger is increased, but the pressure drop is substantially reduced. The increased heat transfer effected by fins may therefore not be worth the price paid by the increased pressure drop. This point can only be answered by a more detailed systems analysis.

CONCLUDING REMARKS

The light-bulb heat-exchanger concept has been investigated as a possible means of using a combustion heat source in conjunction with an inert-gas magnetohydrodynamic (MHD) power generation system. The effects of combustion-gas emissivity, transparent-wall transmissivity, radiation-receiver emissivity, and the use of fins to increase the convective heat transfer to the inert gas were studied.

16

The major effect of reducing the emissivity of the combustion gas was to increase the size of the heat exchanger. A similar effect resulted from decreasing the fin effectiveness in the inert-gas channel. However, in the latter case the inert-gas pressure drop was greatly decreased. This decrease in pressure drop should result in a corresponding decrease in pumping power and hence higher system efficiencies. This trade-off between size and efficiency requires more extensive systems analysis.

The value of the emissivity of the radiation receiver with the range examined, 1.0 to 0.9, had a negligible effect upon the results. The radiation receiver therefore poses no problem concerning the feasibility of the light-bulb heat exchanger for MHD applications.

The critical problem appears to be the transparent wall. In particular, the feasibility of the concept relies to a great extent on the infrared cutoff. The value of the cutoff considered herein is 4.2 micrometers, which is representative of room-temperature fused quartz (ref. 9, pp. 6-58). How this value changes with temperature has not yet been investigated.

The infrared cutoff may become even more critical as a more realistic model of the combustion-gas spectral emissivity is considered. In this analysis we assumed luminous gases, that is, a gray body spectrum. However, under stoichiometric combustion conditions the existence of unburned solid particles throughout the length of the heat exchanger is questionable. If these particles do not persist, one must rely on the radiation from H_2O and CO_2 bands whose spectrum is in the range of the infrared cutoff considered herein. A further shift of the combustion-gas emission spectra toward the infrared is expected to occur as the result of absorption and reradiation in the cold gas boundary layers near the transparent wall.

While the analysis carried out in this report indicates the possible feasibility of the light-bulb heat-exchanger concept, there are still a large number of questions to be answered. The primary need is for a detailed systems analysis. This is required not only to determine the competitiveness of the heat-exchanger, inert-gas MHD system as compared to direct MHD conversion with a combustion generator, but also to determine the required operating range of the heat exchanger and the optical properties of the transparent wall. If further analysis indicates that the system is competitive, a more rigorous treatment of the spectral emissivity of the combustion gas and the transmissivity of the transparent wall is in order.

Lewis Research Center,
National Aeronautics and Space Administration,
Cleveland, Ohio, September 12, 1973,
503-10.

APPENDIX - SYMBOLS

C_p specific heat at constant pressure

f friction factor

H total emissive power of a black body between λ_{min} and λ_{max}

h film coefficient for convective heat transfer

K thermal conductivity

M Mach number

$\dot{m}$ mass flow rate

P pressure

q_{gc} heat flux from combustion gas due to convection

q_{gr} net heat flux from combustion gas due to radiation

q_{1r} net radiant heat flux into transparent wall

q_{3c} convective heat flux into inert gas from hot wall of radiation receiver

q_{4c} convective heat flux into inert gas from cool wall of radiation receiver

q_{2r} net radiant heat flux into radiation receiver

q_{4r} net radiant heat flux across inert gas channel to cool wall of radiation receiver

q_{23} conductive heat flux through inner wall of radiation receiver

R radius

r reflectivity

T temperature

$\overline{T}$ recovery temperature

v velocity

x axial distance along heat exchanger

W_{23} thickness of inner wall of radiation receiver

W_{34} width of inert-gas coolant passage

α absorptivity

δQ volume heat loss

$\delta \underline{X}$ friction force

γ ratio of specific heats

ϵ	emissivity
η	factor accounting for increased convective heat transfer due to fins
Λ_P	defined by eq. (11)
Λ_T	defined by eq. (12)
$\lambda_{min}, \lambda_{max}$	wavelength cutoffs of transparent wall
ρ	mass density
σ	Stefan-Boltzmann constant
τ	transmissivity

Subscripts:

c	convective heat transfer
g	combustion gas
i	inert gas
r	radiation receiver

Other subscripts are defined in figure 3.

REFERENCES

1. McLafferty, G. H.: Survey of Advanced Concepts in Nuclear Propulsion. J. Spacecraft and Rockets, vol. 5, no. 10, Oct. 1968, pp. 1121-1128.

2. Merson, R. H.: An Operational Method for the Study of Integration Processes. Proceedings of a Symposium on Data Processing, Weapons Research Establishment, Salisbury, South Australia, 1957, p. 24.

3. Gordon, Sanford; and McBride, Bonnie J.: Computer Program for Calculation of Complex Chemical Equilibrium Compositions, Rocket Performance, Incident and Reflected Shocks, and Chapman-Jouguet Detonations. NASA SP-273, 1971.

4. Hirschfelder, Joseph O.; Curtiss, Charles F.; and Bird, R. Byron: Molecular Theory of Gases and Liquids. John Wiley & Sons, Inc., 1954.

5. Way, S.: MHD Power Plant for Early Realization. Fifth International Conference on Magnetohydrodynamic Electrical Power Generation, Vol. 1, Munich, 1971, p. 615-628.

6. Nichols, Lester D.: Combined Turbine-Magnetohydrodynamic Brayton Cycle Power System for Space and Ground Use. NASA TN D-6513, 1971.

7. Jakob, Max: Heat Transfer. Vol. II. John Wiley & Sons, Inc., 1957.

8. Chandrasekhav, Subrahmanyan: Radiative Transfer. Dover Publications, Inc., 1960.

9. McCarthy, Kathryn A.; Ballard, Stanley S.; and Wolfe, William L.: Transmission and Absorption of Special Crystals and Certain Glasses. American Institute of Physics Handbook. Second ed., McGraw-Hill Book Co., Inc., 1963, pp. 6-45-6-78.

TABLE I. - OPERATING PARAMETERS FOR CASES ANALYZED

[Inlet stagnation conditions of combustion gas: P_g = 10 atm, T_g = 3200 K; exit stagnation conditions of inert gas: P_i = 10 atm, T_i = 2500 K; diameter of combustion gas duct, 2 meters; diameter of radiation receiver, 6 meters; minimum wavelength cutoff of transparent wall, 0.2 micrometers. Blanks denote that those values are the same as the first case.]

Case	Combustion-gas mass flow rate, $\dot{m}_g$ kg/sec	Combustion-gas emissivity, ϵ_g	transparent Wall Transmissivity, τ_1	Maximum wavelength cutoff of transparent wall, λ_{max}, μm	Radiation-receiver emissivity, ϵ_r	Factor accounting for increased convective heat transfer due to fins, η	Inert gas mass flow rate, $\dot{m}_i$, kg/sec	Inert gas pressure drop/Outlet pressure	Length beyond which heat exchanger is ineffective, L, m	Thermal input, MW	MHD input, MW	Wall input, MW	Efficiency, percent
1	38.5	1	1	4.2	1	5	243.9	0.076	15	345	210	23.8	52.2 49.5
2	-----	- -	- -	- -	- -	- -	176.7	0.060	- -	-----	151.9	20.8	48.8 46.6
3	26.95	0.6	- -	- -	- -	- -	166.3	0.075	- -	241.5	143	17.7	51.8 49.0
4	-----	- -	0.9	- -	- -	- -	197.9	0.072	- -	-----	170	57.0	50.0 43.3
5	-----	- -	- -	3.0	- -	- -	197.9	0.070	- -	-----	170	51.3	50.0 44.0
6	-----	- -	- -	- -	0.9	- -	-----	-----	- -	-----	- -	----	---
7	-----	- -	- -	- -	- -	2.5	-----	0.047	18	-----	- -	30.4	52.0 48.5

21

Figure 1. - Conceptual configuration of light-bulb heat exchanger.
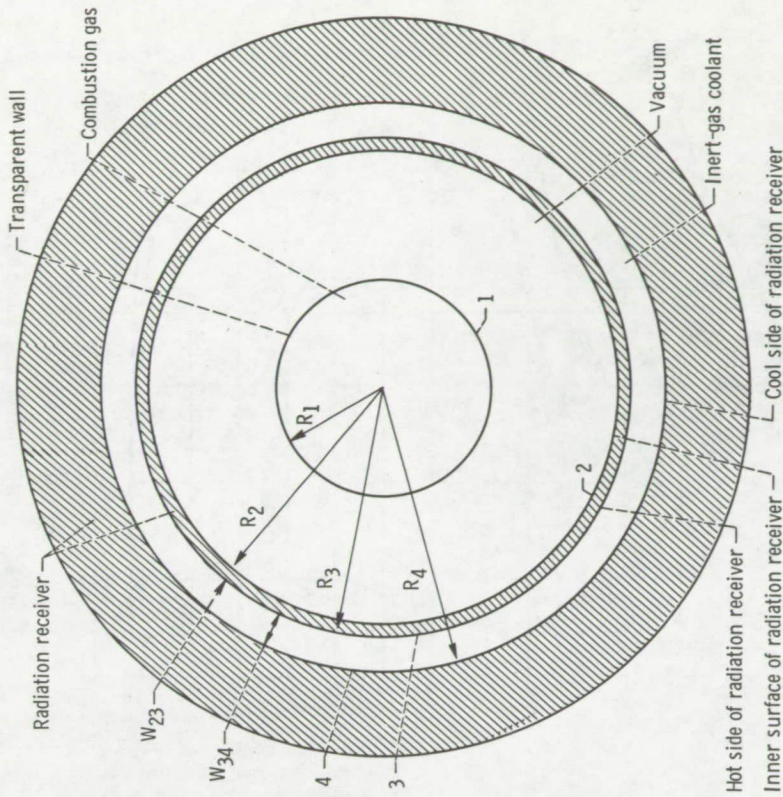
Figure 3. – Light-bulb heat-exchanger model for mathematical analysis. Numbers refer to subscripts used to denote location at which quantities in mathematical analysis are evaluated.
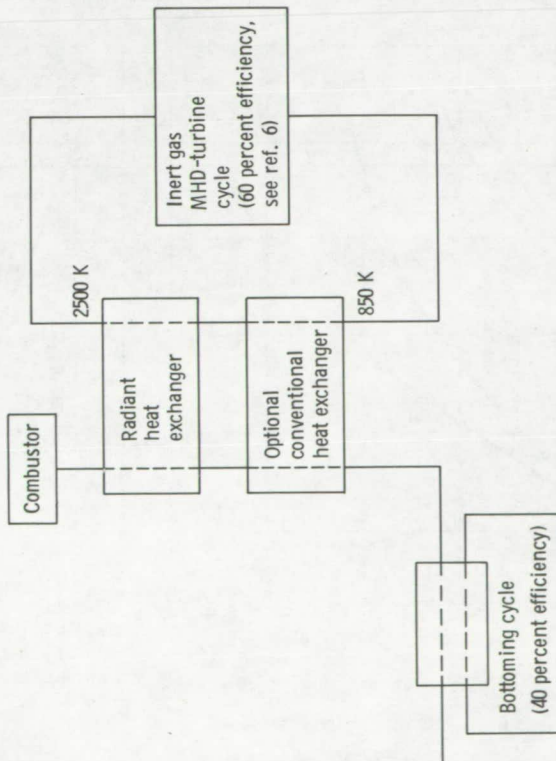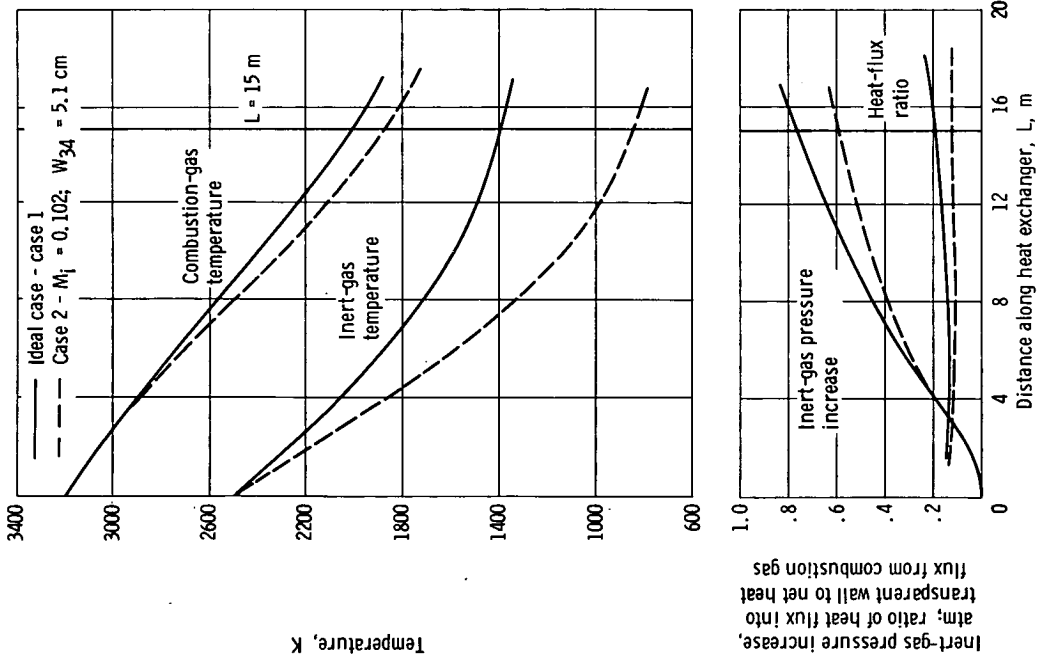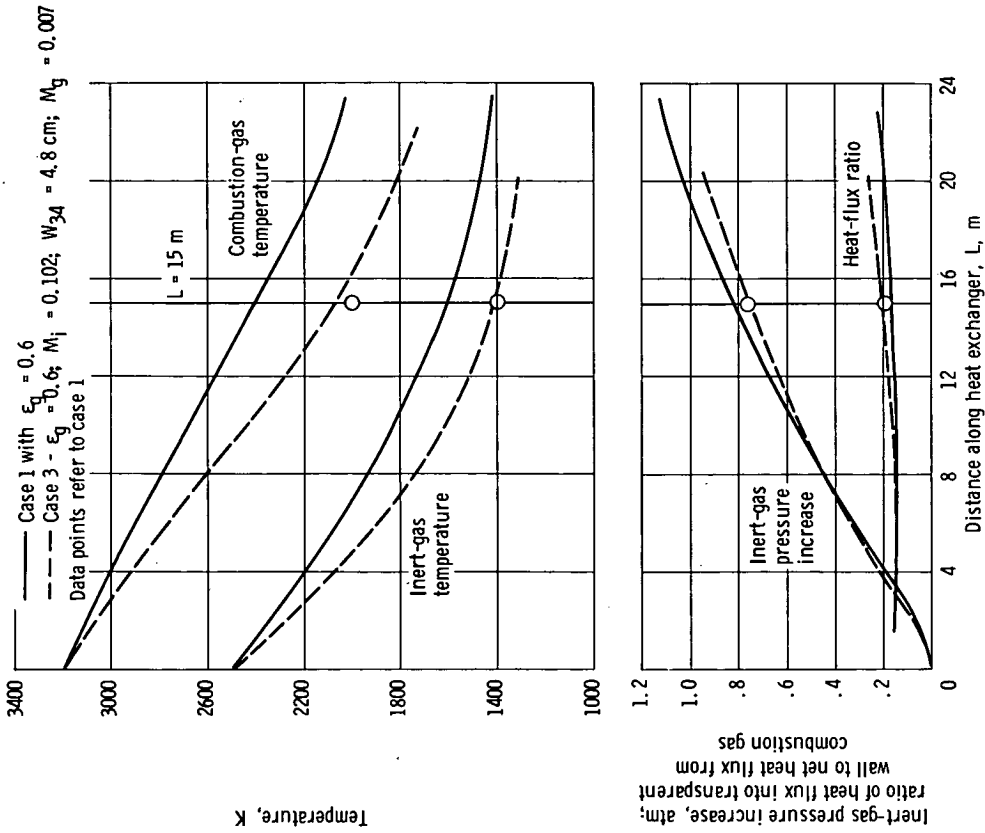

Figure 2. – Schematic of thermodynamic cycle.

Figure 5. - Heat-exchanger performance for case 1 with combustion-gas emissivity ε_g of 0.6 and for case 3 - combustion-gas emissivity ε_g of 0.6, inert-gas Mach number M_i of 0.102, inert-gas channel width W_{34} of 4.8 centimeters, and combustion-gas Mach number M_g of 0.007.

Figure 4. - Heat-exchanger performance for ideal case (case 1) and for case 2 - inert-gas Mach number M_i of 0.102 and inert-gas channel width W_{34} of 5.1 centimeters.

Figure 6. - Heat-exchanger performance for case 1 with radiative transmissivity τ_1 of 0.9 and for case 4 - radiative transmissivity τ_1 of 0.9, inert-gas Mach number M_i of 0.108, and inert-gas channel width W_{34} of 5.4 centimeters.
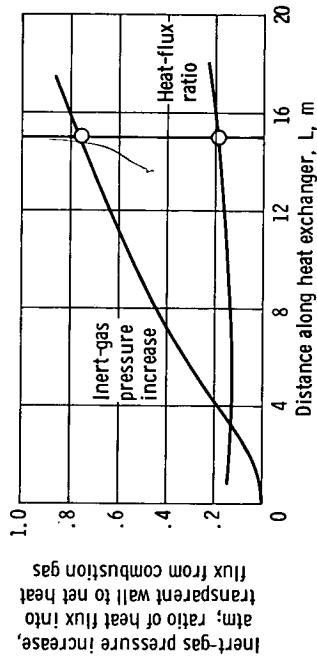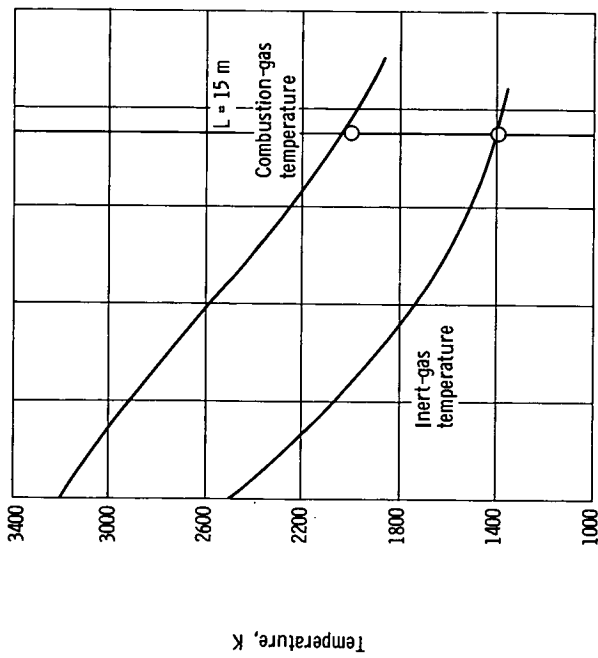

Figure 7. - Heat-exchanger performance for case 1 with maximum infrared cutoff λ_{max} of 3 micrometers and for case 5 - maximum infrared cutoff λ_{max} of 3 centimeters, inert-gas Mach number M_i of 0.108, and inert-gas channel width W_{34} of 5.4 centimeters.
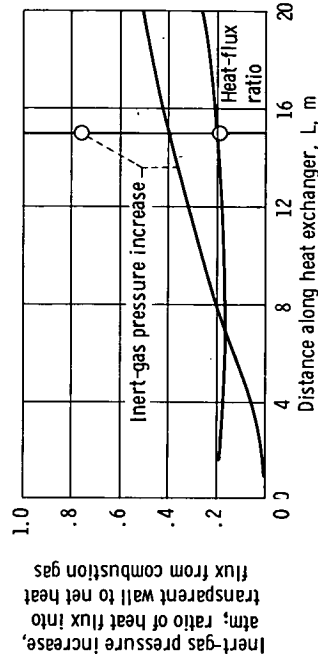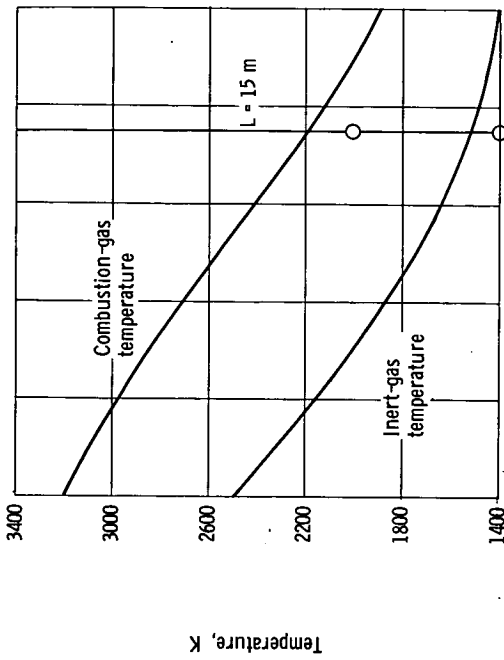
Figure 9. – Heat-exchanger performance for case 7 – factor accounting for increased heat transfer due to fins η of 2.5. Data points refer to case 1.

Figure 8. – Heat-exchanger performance for case 6 – radiation receiver emissivity ϵ_r of 0.9. Data points refer to case 1.

"The aeronautical and space activities of the United States shall be conducted so as to contribute . . . to the expansion of human knowledge of phenomena in the atmosphere and space. The Administration shall provide for the widest practicable and appropriate dissemination of information concerning its activities and the results thereof."
—NATIONAL AERONAUTICS AND SPACE ACT OF 1958

NASA SCIENTIFIC AND TECHNICAL PUBLICATIONS

TECHNICAL REPORTS: Scientific and technical information considered important, complete, and a lasting contribution to existing knowledge.

TECHNICAL NOTES: Information less broad in scope but nevertheless of importance as a contribution to existing knowledge.

TECHNICAL MEMORANDUMS: Information receiving limited distribution because of preliminary data, security classification, or other reasons. Also includes conference proceedings with either limited or unlimited distribution.

CONTRACTOR REPORTS: Scientific and technical information generated under a NASA contract or grant and considered an important contribution to existing knowledge.

TECHNICAL TRANSLATIONS: Information published in a foreign language considered to merit NASA distribution in English.

SPECIAL PUBLICATIONS: Information derived from or of value to NASA activities. Publications include final reports of major projects, monographs, data compilations, handbooks, sourcebooks, and special bibliographies.

TECHNOLOGY UTILIZATION PUBLICATIONS: Information on technology used by NASA that may be of particular interest in commercial and other non-aerospace applications. Publications include Tech Briefs, Technology Utilization Reports and Technology Surveys.

Details on the availability of these publications may be obtained from:

SCIENTIFIC AND TECHNICAL INFORMATION OFFICE

NATIONAL AERONAUTICS AND SPACE ADMINISTRATION

Washington, D.C. 20546